Inorganica Chimica Acta, 146 (1988) 37–53

Geometry Determination for AL_n Systems: Principles and Application

ALISON RODGER and BRIAN F. G. JOHNSON

University Chemical Laboratory, Lensfield Road, Cambridge CB2 1EW, U.K.

(Received September 11, 1987)

Abstract

The question of determining the geometry of AL_n systems is approached by examining the interactions within a molecule. The consequences of assuming that L–L interactions dominate the orientation of Ls around A in AL_n are explored. Successful application to a wide range of AL_2, AL_3, AL_4, AL_5, AL_6, lithium oxides and xenon compounds, including excited states, radicals and charged systems is presented.

I. Introduction

A range of shapes of different symmetries as well as different bond angles and bond lengths can be adopted by a molecule with the formula $AL_n, n > 1$. Various rationalizations exist to account for the structures which are observed in covalently bonded main group systems. However, for molecules where A is a transition metal, or where the A–L bond is significantly ionic the situation is less satisfactory. Valence Shell Electron Pair Repulsion (VSEPR) Theory [1], or non-bonding radii [2], or a variety of qualitative molecular orbital (MO) arguments [3] may or may not provide an explanation. Of course, a quantitative MO or valence bond calculation will, in principle, determine the stable geometries of a particular system. Such a calculation is, however, seldom feasible for a transition metal complex or for molecules involving larger main group elements. Ideally one would like a simple and general model for determining the geometry of an AL_n system. In practice, simplicity and complete accuracy are seldom compatible, so a more realistic aim would be the determination of the approximate geometry of any AL_n system by a model which, in principle, could be extended to provide an accurate geometry at the expense of simplicity. The importance of this point must not be underestimated; a model which cannot be extended, at least in principle, to being an accurate representation of the system is probably not representing the system on any level. Having stated our aim we shall begin with a brief discussion of the reasons why currently available models either fail for some systems or are not satisfactory for other reasons.

Some molecular structure models endeavour to determine the value of n for which the combination AL_n is most stable, others address the question of determining the most stable geometry for one A and n Ls. Various electron counting rules, such as the octet rule for main group elements and the eighteen electron rule for transition metals [4] determine n correctly in AL_n compounds sufficiently often to suggest that electron count is one criterion for stability. The exceptions which exist suggest that there are other factors which contribute to compound stability. Even within the first row elements the existence of Li_nO compounds for $n > 2$ suggests that more than eight electrons can be accommodated, and BF_3 shows that fewer than eight electrons may make a stable compound. Other methods for determining n for which the combination AL_n is stable involve determining the energy of AL_n as a function of n (which also involves determining the geometry of the most stable AL_n for each n). Because of its computational utility, MO theory at various levels of approximation is the most commonly used tool for this purpose though its utility is limited to comparatively small systems. Valence bond based approaches (including generalized valence bond theory, and various group functional approaches [5]) provide alternative approaches which are currently less computationally convenient but which may prove more appropriate than MO theory for some systems. The simplified group functional approach of Schipper [5] shows promise for transition metal complexes in this regard.

If rather than determining n one wishes to concentrate on determining the most stable AL_n geometry for a given n, then a semi-quantitative or more qualitative approach may be sufficient. Frequently the molecular formula of a system can be determined experimentally long before its geometry (especially in fluid phases) can be ascertained, so it is often desirable to have a simple way of deriving the most probable geometry or geometries. Currently the safest way to proceed is via one of the various qualitative MO approaches whose basis is well established, such as Walsh diagrams or the 'Jahn–Teller approaches' of Burdett [3]. (Burdett's work is based on considering the first and second order terms in the perturbation

0020-1693/88/$3.50

expansion of the potential energy of the system, and determining from an MO energy level diagram and the symmetries of the vibrations of the system whether any vibration causes a net reduction in the energy of the system.) An approach based on MO theory can clearly be extended, at least in principle, to give an accurate answer if required. In practice problems arise with qualitative MO approaches when it is not possible to determine, by inspection, whether the net energy change on altering a geometry is positive or negative. Sometimes a semiquantitative determination of the changes in overlap integrals between atomic orbitals results in a sufficiently accurate estimate of the changes in energy upon changing geometry, otherwise a proper MO calculation is required. Unfortunately it is difficult to extract general principles from a full MO calculation, so each system must be treated on its own merits. In addition the nature of the MO formalism means that as soon as any calculation, even at the SCF level, is performed, full exchange symmetry is introduced. Most of the exchange symmetry makes only a small contribution to the energy of the system, so for a question requiring only a semiquantitative answer, there is an increase in the size of the calculation to little effect. This is, however, inescapable with MO theory and is part of the reason why an alternative formalism which introduces full exchange symmetry at a later stage of the calculation may be preferable for some tasks [5].

A more qualitative and simpler model which has been used to rationalize the geometries of a wide range of covalent main group molecules is the Valence Shell Electron Pair Repulsion Scheme (VSEPR) [1]. VSEPR has intuitive appeal to chemists brought up on two-electron bonds, pairs of electrons of opposite spin and the Pauli exclusion principle. It involves dividing the valence shell electrons into pairs and then determining the geometry by minimizing the repulsion between the pairs, the repulsion of lone pairs and double and triple bonds being larger than that of a single bond, and the repulsion of a single bond decreasing with increasing electronegativity of the ligand it connects to the central atom. Even if we grant some physical reality to the concept of lone pairs of electrons, the question remains whether the electron pair repulsion is a dominant factor determining geometry. We shall return to this point after considering the factors which contribute to the total bonding energy of an AL_n system when we shall endeavour to see why VSEPR works when it does (many main group covalently bonded systems) and why it fails at other times (transition metal systems and ionically bonded systems). The aim of this work is to provide an alternative, or perhaps an extension, to VSEPR which works for most AL_n type systems, whether ionic or covalent, ground state or excited state, even number or odd number of electrons, and whose exceptions are understood.

Let us consider a hypothetical stepwise formation of the molecule AL_n from its component parts. The electron density of an isolated A is spherical. When an L approaches closely enough to A to interact, A's electron density is distorted so as to ensure that there is enough electron density in the A–L bonding region to form a bond, and the remaining electron density relaxes to its most stable configuration. The same thing happens with each additional L. The energy of the final system can be approximated by the sum of the contributions from the A–L interactions, the L–L interactions (we include in L the region between A and L), and the effect of the residual (*i.e.* nonbonding valence shell) electron density. There will be an interplay of all these forces. The A–L interaction, which is the most stabilizing, is maximized for a certain bond length. Thus the most stable AL_n system will have as many ligands as it has electrons to make stable bonds, unless this results in large L–L repulsive interactions due to overcrowding. If n is too large for the ligands to fit comfortably around A at the optimal bond length, then the A–L bond length will be increased, perhaps to the extent that the loss in stabilization energy per bond is $\sim 1/n$ th of the bond energy, in which case AL_{n-1} is more stable than AL_n. In practice first row A have a maximum of 4 L, second and third a maximum of 6, and larger A seldom have more than 8 or 9. Let us assume that the A–L bond strength is essentially independent of the relative orientations of the L (we shall return to this below). The L–L interactions and the effect of nonbonding electron density on A then determine the orientation of the L about A. Within this discussion we can see that VSEPR theory takes the next most important energetic contribution to be that from the residual electrons – it assumes that their most stable conformation is as lone electron pairs (if possible). Then it assumes that the next largest energetic effect is the repulsion of the electrons in bonds and in lone pairs. These assumptions clearly break down for very ionic systems e.g. Li_2O, which is probably more correctly thought of as $Li^+_2O^{2-}$ [3] with the L–L charge–charge repulsion dominating the geometry. In addition, neither the VSEPR nor a charge modification account for the square pyramidal geometries of SbF_5 and $SbPh_5$ and the bent geometries of SrF_2 etc. (see below). Problems also arise for transition metals which can perhaps be ascribed to the problem of determining the valence electrons. This suggests that the VSEPR model may also give the 'right' answers for the wrong reasons in some other instances. If on the other hand we decide that the L–L interactions (their form as yet unspecified) are usually the most significant determiners of AL_n geometry then we are assuming that the residual electrons can adopt a configuration which (under any

circumstances) differs from its optimum configuration by less than the L–L interaction.

In this work we shall explore the consequence of assuming that the L–L interaction dominates the orientation of the Ls around A in AL_n. Before proceeding, however, we should consider the earlier assumption that A–L bond strength is independent of the orientations of the Ls. This is obviously not completely true, the environment of a bond does affect its strength, but it may be sufficiently accurate for our purposes. An A–L bond will be weakened by a number of factors which are determined by the relative positions of the Ls. Firstly, the factor mentioned above that although the L–L interaction is assumed to be weaker than the A–L interaction, should a proposed geometry require Ls to approach too closely (say within a hard sphere radius) then the L–L interaction will dominate, forcing the A–L bond to lengthen and thus weaken. An A–L bond will also be weaker in one geometry compared with another if it has less bonding electron density in one. For example the C–O bond of formaldehyde is much stronger than that of methanoate due to the availability of only one carbon electron for C–O bonding in methanoate and two in formaldehyde. This idea may also be relevant in 'electron deficient' systems such as boron. BH_3 is calculated to be a planar geometry [6], yet the L–L interaction (see below) favours a pyramidal geometry such as is observed in NH_3. In BH_3 a pyramidal geometry with ~two-electron bonds would require all the valence shell electron density to be concentrated on one side of the boron. Such an electron distribution may be sufficiently energetically unfavourable for some of the valence shell electron density to not take part in the bonding of a pyramidal BH_3 whereas all of it would be involved in the bonds of a planar BH_3. In fact BH_3 does not exist as a stable species, it always dimerizes to form B_2H_6 (AlH_3 behaves analogously), which suggests that the net effect of the above discussion is to render BH_3 not sufficiently stable to exist. BF_3 by way of contrast is a stable compound due to the charge interactions which favour a trigonal planar geometry. We shall consider these systems further in section III. Bond angles of less than 90° are also considered in section III.

II. Ligand–Ligand Interactions

The geometries favoured by the ligand–ligand interactions of a molecule are those which minimize any repulsive forces and maximize attractive ones. The short range L–L interaction is dominated by repulsion due to overlapping of electron density on the two Ls. For our purposes this repulsion can be modelled by a hard sphere radius (more accurate descriptions can be achieved by a better short range potential) which defines minimum nearest neighbour distances. We then assume that the intermediate and long-range L–L interaction is not exchange dominated, so that electrostatic interactions provide an adequate description. Perturbation theory can be used to expand the electrostatic interaction in a series of different terms with varying r^{-n} dependence.

If L is uncharged, then the dispersion energy is the dominant L–L interaction term. The dispersion energy due to the interaction of two ligands is approximately [7]

$$E_{\text{disp}}(L_1 - L_2) \approx -3/2 E_{12} \alpha_1 \alpha_2 r_{12}^{-6} \quad (1)$$

where r_{12} is the L_1–L_2 distance, α_i is the polarizability of L_i, and $E_{12} = E_1 E_2/(E_1 + E_2)$ where E_i is an average excitation energy of L_i (the ionization energy of L_i is usually a sufficiently good value for E_i). Thus a given L–L interaction is most stabilizing (*i.e.* most negative) for uncharged L if the L–L distance is as small as possible, *i.e.* if the L–L distance equals the sum of the L hard sphere radii. Thus for the total L–L interaction to be maximally stabilizing, all Ls are brought as close together as possible. At this stage it is appropriate to note that this provides a justification for the success of the 'non-bonded radii' approach to molecular geometry taken by Bartell [2] and later by Glidewell [8]. In the next section we shall explore the various geometries which result from the maximization of dispersion interactions subject to a hard sphere radii on the ligands.

If the L are charged, either intrinsically or due to an ionic bond to A providing a partial charge, then the charge interaction may become a significant factor in determining the geometry of a system. The energy due to the interaction of two charged ligands is

$$E_{\text{ch}}(L_1 - L_2) = q_1 q_2 / r_{12} \quad (2)$$

where q_i is the charge on L_i and r_{12} is the L–L distance. $E_{\text{ch}}(L_1 - L_2)$ can be negative (*i.e.* stabilizing) if L_1 and L_2 have opposite charges. In such a case the charge interaction tends to bring the Ls as close together as possible. In most instances of interest to us in this work the charge interaction is positive and so destabilizing. It tends to push the L apart, thus opposing the effect of the dispersion interaction.

The observed geometry in a system with charged Ls is then a balance between the dispersion determined geometry and the charge determined geometry. Ideally some quantitative estimate of the relative significance of the two terms is required. The ratio of the two energy terms is

$$E_{\text{disp}}(L_1 - L_2)/E_{\text{ch}}(L_1 - L_2) \approx 1.080 E_{12} \alpha_1 \alpha_2 / (r_{12}^5 q_1 q_2) \quad (3)$$

where E_{12} is in MJ mol^{-1}, r_{12} is in Å, α_i is in Å^3 and q_i are in units of electronic charge. The degree of elec-

TABLE I. Some Polarizabilities and Dipoles

Compound	Dipole (D)[a]	q (e)[b]	Fragment	Polarizability ($Å^3$)[c]
HF	1.91	0.43	F^-	0.96
HCl	1.08	0.18	Cl^-	3.60
HBr	0.79	0.12	Br^-	5.0
HI	0.38	0.049	I^-/I	7.6/4.96
LiH	5.828	0.76	Li^+/Li	0.03/22[d]
LiF	6.38	0.84	H^-	10.18
LiCl	7.08	0.729	He	0.20
NaCl	8.97	0.79	Na^+/Na	0.19/21.5
ClF	0.85	0.108	Ne	0.40
BH	1.27	0.22	Cs^+/Cs	2.6/42.0
BF	0.5 ± 0.2	0.079	CH_2	2.099
AlF	1.53	0.195	O^{2-}	2.74
CO	0.112	0.021	S^{2-}	8.94
CS	1.97	0.27	CO	1.95[e]
SiO	3.09	0.56	CN^-	3.47[f]
SiS	1.74	0.17	OH^-	1.95[f]

[a]Data from ref. 9. [b]q is the partial charge on the atoms, in units of electronic charge. q is determined from the dipole by dividing it by 4.80298 times the bond length. Bond lengths from refs. 6 and 10. [c]Data from ref. 11. [d]Data from ref. 12. [e]Datum from ref. 13. [f]Data from ref. 14.

tron transfer across the A–L bond can be determined from the bond dipole (dipoles of some diatomic molecules are given in Table I). Alternatively the degree of electron transfer is approximately related to the electronegativity difference of the ligands. Some polarizabilities are also given in Table I. E_{12} is of the order of 1, α_i is approximately the volume of L, r_{12} is about two times a non-bonded radius, *i.e.* 2–4 Å. It is thus possible to make some estimate of eqn. (3). In most of the systems we shall be examining the dispersion term is the larger, however the geometry is frequently modified by charge interactions as we shall see. Ligands with large charge and small polarizability, such as Li^+ have their geometry dominated by charge interactions.

II.1. Geometries Which Optimize L–L Dispersion Interactions

In this subsection and the next we shall consider the somewhat abstract question of which geometries are favoured by dispersion and charge interactions. The conclusions are illustrated in Figs. 1 to 6. Applications which further illustrate and clarify the conclusions are contained in section III. The L–L dispersion is attractive, so it is maximally stabilizing when it has the largest magnitude possible, so our aim is to determine what geometries maximize the dispersion interaction.

AL_2

AL_1L_2 is the simplest molecule for which ligand interactions are operative. The L_1–L_2 dispersive interaction is maximized when the distance between

Fig. 1. Geometry adopted by AL_2 molecules. A is indicated by a square and the L by circles. ρ is the optimal A–L bond length, r is the inter-ligand distance, θ is the LAL bond angle. The bent geometry is favoured by dispersion interactions and attractive charge interactions for ligands which are small compared with the A–L bond lengths. The linear geometry is favoured by repulsive charge interactions and large ligands.

L_1 and L_2, r_{12}, is as small as possible. There are three situations which must be considered.

(i) If $R_1 + R_2 < \rho_1 + \rho_2$ where R_1 and R_2 are the hard sphere radii of L_1 and L_2 respectively, and ρ_1 and ρ_2 are the optimal bond lengths for A–L_1 and A–L_2, then the geometry will be bent, with the bond angle,

$$\theta = \cos^{-1}\{[(R_1 + R_2)^2 - \rho_1^2 - \rho_2^2]/[2\rho_1\rho_2]\} \quad (4)$$

as is illustrated in Fig. 1. When $L_1 = L_2$ then eqn. (4) simplifies to $\theta = 2\sin^{-1}(R/\rho)$.

(ii) If $R_1 + R_2 = \rho_1 + \rho_2$, then the geometry will be linear.

(iii) If $R_1 + R_2 > \rho_1 + \rho_2$ then AL_1L_2 cannot be formed with the A–L_1, A–L_2 bond lengths at their optimal values. So either the bonds stretch to accommodate the size of the ligands, and probably form a linear molecule or else AL_1L_2 is not sufficiently stable to exist and it is not observed.

AL_3

The situation for $AL_1L_2L_3$ is very similar to that for AL_1L_2 since L_i is a nearest neighbour of L_j in any geometry centred on A. Thus the largest dispersion interaction will occur when the ligands are separated only by their hard sphere radii and the bond angles are determined by eqn. (4). For the sake of clarity we shall consider the case where the ligands are identical. Small ligands for which $R_i < \sqrt{3}\rho_i/2$ adopt a C_{3v} trigonal pyramidal (tpy) geometry; ligands for which $R_i = \sqrt{3}\rho_i/2$ adopt a D_{3h} trigonal planar (tpl) geometry; and large ligands for which $R_i > \sqrt{3}\rho_i/2$ either adopt a strained tpl geometry or are not observed. The geometries are illustrated in Fig. 2. Lower symmetry geometries are adopted when the ligands are different.

AL_4

It becomes increasingly notationally complex to consider geometries with different ligands, so we shall concentrate on geometries with identical ligands. The geometries favoured by dispersion interactions for the lower symmetry systems are simply distortions from the higher symmetry ones. The geometries which four ligands around a central atom can adopt fall into the

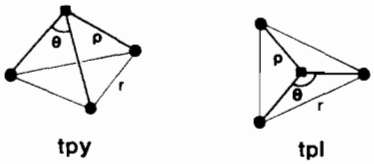

Fig. 2. Geometry adopted by AL_3 molecules. A is indicated by a square and the L by circles. ρ is the optimal A–L bond length, r is the inter-ligand distance, θ is the LAL bond angle. The tpy (trigonal pyramidal) geometry is favoured by dispersion interactions for ligands which are small compared with the A–L bond lengths. The tpl (trigonal planar) geometry is favoured by dispersion interactions for large ligands and by charge interactions. If the ligands have different sizes or charges, a distorted tpl or T shaped structure results.

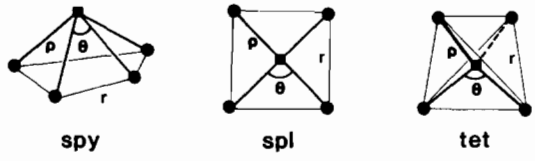

Fig. 3. Geometry adopted by AL_4 molecules. A is indicated by a square and the L by circles. ρ is the optimal A–L bond length, r is the inter-ligand distance, θ is the LAL bond angle. The spy (square pyramidal) geometry is favoured by dispersion interactions for ligands which are small compared with the A–L bond lengths. As ligands increase in size dispersion interactions favour the spl (square planar) geometry, geometries intermediate between the spl and tet (tetrahedral) geometries and finally the tet geometry. Charge interactions favour the same range of structure depending on the relative signs and magnitudes of the charges.

categories of tetrahedral (tet), distorted tetrahedral, square planar (spl) and distorted square planar. We shall begin by comparing the dispersion energies of a tetrahedral geometry in which every ligand interacts with three other ligands, and a square planar geometry in which the ligands can get closer together but only interact significantly with two other ligands.

$$E_{\mathrm{dis}}(\mathrm{tet}) \approx \{-3/4E_{\mathrm{L}}\alpha_{\mathrm{L}}^2\}6r_{ij}(\mathrm{tet})^{-6} \tag{5}$$

$$\text{and } E_{\mathrm{dis}}(\mathrm{spl}) \approx \{-3/4E_{\mathrm{L}}\alpha_{\mathrm{L}}^2\}4r_{ij}(\mathrm{spl})^{-6} \tag{6}$$

where r_{ij} is the distance between two Ls. If AL_4 can adopt a spl geometry without straining the A–L bond, *i.e.* $r_{ij}(\mathrm{spl}) = \sqrt{2}\rho_i > 2R_i$, where ρ_i is the optimal A–L bond length and R_i is the hard sphere radius of a ligand, then the spl geometry is more stable than the tetrahedral geometry which requires $r_{ij}(\mathrm{tet}) = 2\rho_i \sin 109.5^\circ > 2R_i$. However, the tetrahedral geometry can accommodate larger ligands without A–L bond strain. Since the spl geometry can be gradually distorted to become tetrahedral one would expect to see a progression from square planar to tetrahedral with increasing size of ligand. In fact for small ligands maximization of the dispersion interaction will favour a square pyramidal (spy) geometry of C_{4v} symmetry, as illustrated in Fig. 3.

AL_5

AL_5 has two archetypical geometries: the trigonal bipyramid (tbp) of D_{3h} symmetry and the square based pyramid (sbp) of C_{4v} symmetry. The dispersion energies for these two geometries, which are illustrated in Fig. 4, are

$$E_{\mathrm{dis}}(\mathrm{tbp}) \approx \{-3/4E_{\mathrm{L}}\alpha_{\mathrm{L}}^2\}[6r_{\mathrm{a}}(\mathrm{tbp})^{-6} + 3r_{\mathrm{e}}(\mathrm{tbp})^{-6}] \tag{7}$$

and

$$E_{\mathrm{dis}}(\mathrm{sbp}) \approx \{-3/4E_{\mathrm{L}}\alpha_{\mathrm{L}}^2\}[4r_{\mathrm{a}}(\mathrm{sbp})^{-6} + 4r_{\mathrm{b}}(\mathrm{sbp})^{-6}] \tag{8}$$

where e denotes an equatorial, b a basal and a an axial ligand, r_{a} is the distance between an axial and an equatorial/basal ligand, r_{e} between two equatorial ligands and r_{b} between two basal ligands. For molecules which can achieve their optimal bond length, ρ_{L}, $r_{\mathrm{a}}(\mathrm{sbp}) = r_{\mathrm{b}}(\mathrm{sbp}) = r_{\mathrm{e}}(\mathrm{tbp}) = \sqrt{2}\rho_{\mathrm{L}}$, and $r_{\mathrm{e}}(\mathrm{tbp}) = \sqrt{3}\rho_{\mathrm{L}}$ so the sbp geometry is more stable than the tbp. However, if the hard sphere radius is sufficiently large that $\rho_{\mathrm{L}} < \sqrt{2}R_{\mathrm{L}}$, then the tbp geometry becomes increasingly favoured as all the sbp bonds will be strained but only the axial bonds of the tbp will be strained. For small L such that $\rho_{\mathrm{L}} > \sqrt{2}R_{\mathrm{L}}$ a distorted sbp, sbpB, of C_{4v} symmetry (see Fig. 4) which enables the L to be closer together will be favoured. As for the AL_4 geometries a continuous progression between the geometries of Fig. 4 is possible and in fact found (see section III).

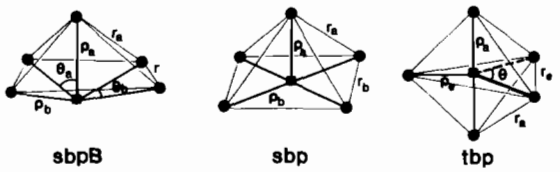

Fig. 4. Geometry adopted by AL_5 molecules. A is indicated by a square and the L by circles. ρ is the optimal A–L bond length, r is the inter-ligand distance, θ is the LAL bond angle. Subscript a denotes axial, subscript b basal, and subscript e equatorial. The sbpB (square based pyramid with A below the plane of the ligands) geometry is favoured by dispersion interactions for ligands which are small compared with the A–L bond lengths. As ligands increase in size dispersion interactions favour the sbp geometry, geometries intermediate between the sbp and tbp (trigonal bipyramidal) geometries, and finally the tbp geometry. Charge interactions favour the same range of structure depending on the relative signs and magnitudes of the charges.

AL_6

The two archetypical geometries for AL_6 are the octahedron (oct) and the triangular prism (tpr). The relevant dispersion energies are

$$E_{dis}(\text{oct } AL_6) \approx \{-3/4E_L\alpha_L^2\}12r_{ij}(\text{oct})^{-6} \quad (9)$$

$$E_{dis}(\text{tpr } AL_6) \approx \{-3/4E_L\alpha_L^2\}[6r_1(\text{tp})^{-6} + 3r_2(\text{tpr})^{-6} + 3r_3(\text{tpr})^{-6}] \quad (10)$$

where r_1 is the L–L distance on the ends, r_2 is the L–L distance on the sides, and $r_3 = \sqrt{(r_1^2 + r_2^2)}$ is the diagonal distance across a rectangular face of the tpr. The A–L distance in an octahedron bears the same relationship to the L–L distance as it does in the square plane and square based pyramid geometries discussed above, *viz.* $r_{ij}(\text{oct}) = \sqrt{2}\rho_L$. One might therefore expect an octahedron or a distorted octahedron to be the geometry favoured by dispersion for small ligands. However, the octahedron is the AL_6 geometry with the largest L–L distance for a given A–L distance, so it is also the most favourable for large L. Thus the geometry predominantly favoured by dispersive interactions for AL_6 is the octahedron. For small ligands a distorted octahedron geometry, rather like a pentagonal bipyramid with an equatorial ligand missing, is the next stage. For even smaller ligands, a tpr geometry will be favoured since the tpr with $r_1 = r_2$, has $\rho_i(\text{tpr}) = \sqrt{7}r_i(\text{tpr})/(2\sqrt{3}) > 1.53R_i$, thus enabling closer approach of ligands.

AL_7

There are three standard geometries for an AL_7 molecule which are illustrated in Fig. 6. The pentagonal bipyramid is favoured for small ligands whose dispersion energy is thus maximized with close packing, though the dispersion energy of the capped octahedron is very similar. Apart from this it is not possible to be conclusive since there is very little difference between the geometries, and small changes in any one of the types of interaction which contribute to the stability of a molecule can result in a different geometry being preferred.

II.2. Geometries which Optimize L–L Charge Interactions

The interactions between the charges on two ligands can be either repulsive or attractive, and within any one molecule with more than two ligands there can be either a mixture of both types of interactions or only repulsive ones. In this section we shall determine the geometries which are favoured by charge interactions. Molecules where all the ligands have the same charge will adopt the geometry which maximizes the interligand distance. The types of geometries adopted by molecules with ligands of different charges can be determined by considering the effect of adding the ligands one at a time.

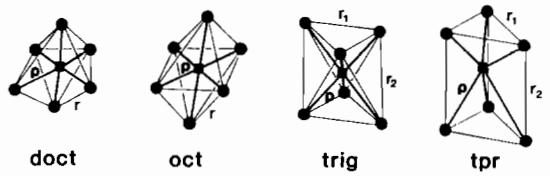

Fig. 5. Geometry adopted by AL_6 molecules. A is indicated by a square and the L by circles. ρ is the optimal A–L bond length, r is the inter-ligand distance, θ is the LAL bond angle. The tpr (triangular prism) geometry is favoured by dispersion interactions for very small and the doct (distorted octahedral) geometry for small ligands. The oct (octahedral) geometry is most commonly found.

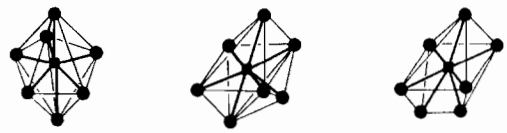

Fig. 6. Geometries adopted by AL_7 systems. Pent = pentagonal bipyramid, coct = capped octahedron and csbp = capped square based prism.

AL_2

An attractive charge interaction will favour a bent geometry with the angle determined by the hard sphere radius for AL_2, and a repulsive interaction will favour a linear geometry. These are illustrated in Fig. 1.

AL_3

Charge interactions in a molecule with three ligands whose charges are identical will adopt the geometry which maximizes the distance between the ligands, *i.e.* tpl (*cf.* Fig. 2).

A molecule with two ligands of the same charge, q_1, and one of charge q_2 has

$$E_{ch}(L_1L_1L_2) = q_1q_2/(\rho \sin\theta/2) + q_2^2/(2\rho \sin\phi/2) \quad (12)$$

where θ is the L_1AL_2 angle, ϕ the L_1AL_1 angle ($\phi = 360^\circ - 2\theta$ for a planar geometry), and for simplicity we have assumed a constant A–L bond length ρ. If q_1 and q_2 are of opposite sign then eqn. (12) is negative (*i.e.* stabilizing) as long as

$$|q_2/q_1| < 2\sin(\phi/2)/\sin(\theta/2) \leqslant 1/(4\cos\theta/2) \quad (13)$$

(the equality holding if the geometry is planar). The geometry favoured by charge interactions when q_1 and q_2 have opposite signs is that which enables θ to be as small as possible (thus θ is determined by hard sphere radii) and ϕ as large as possible while still obeying eqn. (13). Thus we expect to see a distorted planar or T shaped geometry for q_1 and q_2 of opposite sign. If on the other hand q_1 and q_2

are the same sign, the charge interaction is always destabilizing, and is a minimum when the molecule is planar and

$$4q_2 \cos^3\theta/2 + q_1 \cos\theta = 0, \quad \theta > 90^\circ \qquad (14)$$

E_{ch} does not vary much in the region of $\theta = 90^\circ$, so a bond angle of less than 90° may be observed if the dispersion energy favours a smaller angle. We shall return to this below. The geometry the system adopts is the one which maximizes the attraction, and minimizes the repulsion, *i.e.* a T or bent-T shaped geometry with the differently charged ligand at the base of the T.

AL_4

Charge interactions of two positive and two negative ligands will favour a spy or spl geometry, with nearest neighbours of opposite sign and the nearest neighbour distances being determined by hardsphere radii. Exceptions to this may occur for large ligands which cause the A–L bond to be strained. Distortion towards a tetrahedral geometry may then take place.

For one positive and three negative ligands (or the converse), charge interactions will favour a trigonal pyramidal or distorted tetrahedral geometry, with the positive ligand at the apex. Depending on hardsphere radii and relative charge magnitudes, the geometry may be bent so A is slightly below the plane of the three negative ligands.

Charge interactions for four ligands of the same charge will favour a tetrahedral geometry which maximizes their separation.

AL_5

The charge interactions of one positive and four negative ligands will adopt a geometry where the negative ligands favour a tetrahedron which is distorted towards the positive ligand sited in one of the tetrahedral faces. This geometry can equally well be described as a trigonal bipyramid distorted towards one of its apices, which illustrates the arbitrariness of labels given to intermediate geometries.

Charge interactions of two positive and three negative ligands will adopt a distorted trigonal bipyramidal geometry, with the positive ligands at the apices. The degree of distortion will be determined by the relative positive and negative charges since the attractive interactions favour bending the planar ligands until they meet the hard sphere radies of an apical ligand, and the three negative ligands minimize their repulsion when they are in the equatorial plane.

Five ligands with the same charge will favour a tbp geometry *cf.* Fig. 4.

AL_6

The AL_6 geometry favoured by a system with six ligands of the same charge is the octahedron, and just as the attractive dispersion interactions generally result in an octahedron or a distorted octahedron, charge interactions which involve some attractive ones will result in a distorted octahedral-type geometry *cf.* Fig. 4.

III. Applications

In the previous two sections we have examined the types of geometries favoured by dispersion interactions and charge interactions. An additional factor which must be taken into account is whether a particular geometry involves significantly weaker A–L bonds than an alternative geometry. A comparatively weak A–L bond can be identified in a number of ways: (i) if a proposed geometry requires the A–L bond length to fall outside the range of typical A–L bond lengths (*i.e.* a strained geometry); (ii) A–L bonds are either electron deficient or the valence shell electron density is concentrated in one direction. (i) has already been discussed above, and we shall return to (ii) below. An additional restraint is that bond angles of significantly less than 90° are not observed even when predicted by dispersion or charge interactions. We could treat this as a purely empirical rule, however its origin should be able to be traced to an energetic contribution that was ignored in section I. We have been concentrating exclusively on the energetic contributions of inter-ligand dispersion and charge interactions, with some consideration being given to bond strain. In doing this we have completely ignored the factor considered so important in VSEPR theory, namely the repulsion of electrons in bonds. This repulsion becomes more significant when small bond angles force the electrons near the nuclei close together, and probably accounts for the smallest bond angles being about 90°. This repulsion can be viewed as the 'hard sphere' repulsion of the electron density in the bonds. Under normal circumstances it can be ignored because the repulsion of the ligand electron densities prevents the bonds coming close enough together for it to be relevant.

Before proceeding some estimate of hardsphere radii is required. The non-bonding radii of Bartell and Glidewell determined for covalent systems provide a reasonable estimate for a range of compounds. These are given in Table II. If an atom is bonded to another atom of higher electronegativity than four coordinated carbon, then its hard sphere radius will be smaller than the values in Table II, and conversely if bonded to a less electronegative atom.

AL_2

The geometries adopted by AL_2 systems illustrate the principles discussed in the previous sections. Table III contains the data required to predict the dispersion favoured geometry, a table of electro-

TABLE II. Non-bonded Radii (Å) of Bartell [2] and Glidewell [8] Determined from Assuming Covalently Bound Geometries are Determined by Close Packing

					H = 0.92
Be = 1.39	B = 1.33	C = 1.25	N = 1.14	O = 1.13	F = 1.08
	Al = 1.85	Si = 1.55	P = 1.46	S = 1.45	Cl = 1.44
		Ge = 1.58		Se = 1.58	
		Sn = 1.88	Sb = 1.88	Te = 1.87	

negativities (see for example ref. 10) enables an estimate of the relative significance of the charge interactions. Table III also contains the predicted and observed geometries. To a large extent Table III speaks for itself, though some comment is required. Let us begin by considering a typical entry, say BF_2. The A–L bond length, ρ, is 1.31 Å, the hard sphere radius of F will be larger than in say CH_3F, so >1.08 Å, thus the dispersion favoured geometry has a bond angle of >111°. There is probably a little influence from charge interactions, which in isolation would favour a linear structure, so we would predict a slightly larger bond angle than the dispersion favoured angle. The experimental structure in fact has a bond angle of 118°, in accord with this discussion.

The bonding in BeH_2 is essentially covalent so we need only consider the effects of dispersion interactions and the H–Be bond strength. Figure 7 is the calculated electron density for linear BeH_2 and bent BeH_2 [15]. It is interesting to note that the outer electron clouds of the two geometries are approximately superposable about their centres of mass, indicating that it is not energetically favourable for the beryllium to put all its valence shell electrons into bonds when this requires a significant distortion of the electron density. Thus A–L bond strength factors determine the geometry of BeH_2 in accord with the discussions of section I.

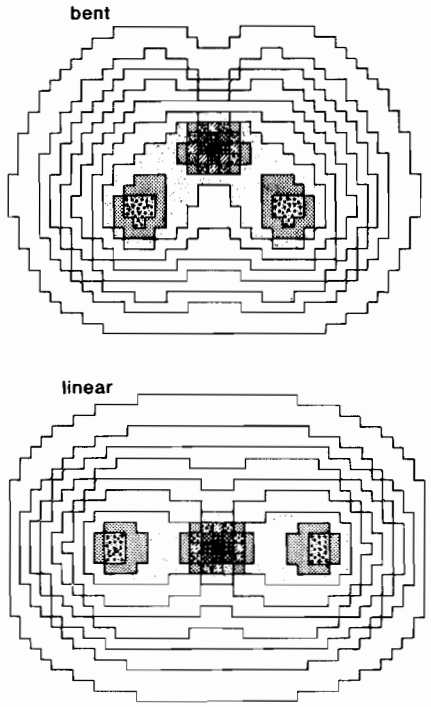

Fig. 7. Electron density maps of bent and linear BeH_2 [15].

Hydrides of the larger atoms have hard sphere radii which are small compared with the bond lengths. A geometry in which hard spheres are in contact then requires a bond angle of much less than 90°, which as discussed above, is not a favourable geometry due to repulsion by the electron density in the bonds. The hydride geometries can then be understood in terms of the discussion of the previous sections. The CH_2 geometries are illustrative. The ground state bond angle is about 10° less than that predicted using the hardsphere radius of H determined from four-coordinate carbon systems. Such a deviation requires only a decrease in the hard sphere radius of H of 0.05 Å from its value of 0.92, which can be understood in terms of the different electron densities on an H when the electron-withdrawing power of the carbon is shared among two hydrogens instead of four hydrogens. The $^3B_1$ state has less electron density on the hydrogens than the ground state, and so a smaller bond angle is favoured by the dispersion interactions, however, the decrease in electron density on the hydrogens results in a positive charge and very small polarizability. Charge interactions then lead to a larger bond angle than in the ground state.

The fluorides all show some effect of charge interactions on the geometry, as expected due to their large electronegativity and small polarizability. It would appear that charge effects are not usually actually dominant in fluoride systems unless they are intrinsically charged. Repulsive charge interactions simply cause the observed bond angle to be greater than that predicted by dispersive interactions alone, and attractive charge interactions (e.g. in HOF) cause it to assume its dispersive geometry since, for linear compounds, both dispersion and attractive charge interactions favour the bond angle being determined by the hard sphere radius.

It is interesting to follow trends in ground state geometry across and down the periodic table. As A

TABLE III. Data Illustrating the Relationship between L–L Interaction Predictions and Experimental Geometries for AL_2 [a]

Compound	ρ (Å)	R (Å)	Geometry favoured by		Experimental	Comment	Reference
			dispersion	charge			
Hydrides							
H–Be–H	1.3	>0.92	$\theta > 90°$		linear (calcn)	A–L	15
H–B–H	1.18	>0.92	$\theta > 102°$		$\theta \approx 131°$		16
H–C–H	1.11	<0.92	$\theta < 112°$		$\theta \approx 102.4$		6
H–C–H, $^3B_1$	1.08	>0.92	$\theta > 117°$	linear	$\theta \approx 136$	charge	6
H–N–H	1.02	<0.92	$\theta < 129°$		$\theta \approx 103.4°$		16
H–N–H$^-$	1.03	<0.92	$\theta < 127$		$\theta = 104°$		6
H–O–H	0.96	$\ll$0.92	$\theta \ll 146°$	linear	$\theta = 105.2°$	*i.e.* R = 0.76	6
H–O–H$^+$ $^2B_1$	1.00	$\ll$0.92	$\theta \ll 134°$	linear	$\theta \approx 110.5°$		6
H–Si–H	1.52	>0.92	$\theta > 75°$		$\theta = 92.1°$	A–L	6
H–P–H	1.43	>0.92	$\theta > 80°$		$\theta = 91.5°$	A–L	16
H–S–H	1.34	0.92	$\theta \approx 87°$		$\theta = 92.1°$	A–L	6
H–Se–H	1.46	0.92	$\theta \approx 78°$		$\theta = 90.6°$	A–L	6
H–Te–H	1.66	>0.92	$\theta > 67°$		$\theta = 90.3°$		6
Fluorides							
F–H–F$^-$	1.13/4	>1.08	$\theta > 143$	linear	linear	charge dom.	6
F–B–F	1.31	>1.08	$\theta > 111°$	linear	$\theta = 118°$	little charge	6
F–O–F	1.41	<1.08	$\theta < 99°$		$\theta = 103.1°$		6
F–Si–F	1.58	>1.08	$\theta > 86°$	linear	$\theta = 108.3°$	charge	6
F–P–F	1.55	>1.08	$\theta > 88°$	linear	$\theta = 97.7°$	charge	6
F–S–F	1.59	1.08	$\theta \approx 86°$	linear	$\theta = 98.2°$	charge	6
F–Zn–F	1.81	>1.08	$\theta > 73°$	linear	linear	charge dom.	17
F–Be–F			bent	linear	linear	A–L	17
F–Mg–F			bent	linear	linear	A–L	17
F–Ca–F			bent	linear	140°	disp. dom.	17
F–Sr–F			bent	linear	108°	disp. dom.	17
F–Ba–F			bent	linear	100°	disp. dom.	17
Oxides and nitrides							
O–C–O	1.22	>1.13	$\theta > 136°$		linear	A–L	10
O–O–O	1.28	<1.13	$\theta < 124°$		$\theta = 116.8°$	disp. dom.	6
O–N–O	$\approx$1.23	$\approx$1.14	$\theta \approx 136°$		$\theta = 134°$		6
O–N–O$^+$	1.15	$\approx$1.14	$\theta \approx 165°$	linear	linear	charge	6
O–N–O$^-$	1.24 ± ?	$\approx$1.14	$\theta \approx 134° \pm ?$	linear	115.4° ± ?		6
N–N–N$^-$	$\approx$1.10	$\approx$1.14	linear	linear	linear with long bond length		6
Chlorides and sulfides							
Cl–O–Cl	1.7	<1.44	$\theta < 115°$		$\theta = 110.9°$		6
Cl–S–Cl	2.014	>1.44	$\theta > 91°$		$\theta = 102.7°$		6
S–C–S	1.6	1.45	$\theta > 130°$		linear	A–L	10
Mixed ligands[b]							
H–O–F	0.97, 1.44		$\theta < 111°$	bent	$\theta = 96°$	charge + disp.	6
H–C–N	1.08, 1.16		$\theta \approx 142°$		linear	A–L	6
H–N–C	1.01, 1.16		$\theta \approx 180°$		linear	A–L	6
H–C–P	1.08, 1.54		$\theta \approx 130°$		linear	A–L	6
H–N–O	1.06, 1.21		$\theta < 129$		$\theta = 108.6°$		6
H–P–O	1.43, 1.51		$\theta > 88°$		$\theta = 104.7°$		6
H–O–Cl	0.98, 1.69		$\theta < 122°$	bent	$\theta = 102.5°$		6
O–C–F	$\approx$1.22, $\approx$1.38		$\theta \approx 116°$	linear	$\theta = 126°$		6
N–S–F	1.45, 1.64		$\theta > 92°$		$\theta = 116.9°$		6
O–N–Cl	1.21, 1.97		$\theta > 105°$	linear	$\theta = 113.3°$		6

(continued)

TABLE III. *(continued)*

Compound	ρ (Å)	R (Å)	Geometry favoured by		Experimental	Comment	Reference
			dispersion	charge			
Metallic A							
$CN-Ag-CN^-$	3.29	≈1.25	bent	linear	linear	charge dom.	10
$Zn(CH_3)_2$	1.929	≈2	linear		linear		6
$Cd(CH_3)_2$	2.112	≈2	linear		linear		6

[a]ρ is the A–L bond length, R is the L hard sphere radius, θ is the LAL bond angle. In the comments column, A–L means either that the experimental geometry is different from the dispersion/charge predicted one due to weaker A–L bonds in the geometry predicted by considering only L–L interactions, or that the bond angle is too small to be observed (see text). Charge indicates that charge interactions have some influence on the structure, dom = dominant, disp = dispersion. [b]See Table II for R values.

goes down any period, the dispersion energy favours a smaller LAL angle, since the bond length increases and the hard sphere radii of L increase only slightly (due to decrease in electronegativity of A). As A goes across a period, its electronegativity increases so the hard sphere radius of L decreases and the A–L bond length decreases. Both effects result in an increase in θ being favoured by dispersion. As L goes down the table the main factor is an increase in its size, so an increase in θ is favoured by dispersion interactions. As L goes across a period, it decreases in size and θ decreases. The effect of charge interactions depends on the degree of charge transfer between A and L; if this increases then charge effects become more significant, if it decreases then less significant. All these trends can be observed in Table III.

The alkali earth halides provide a series of compounds which illustrates the interaction of repulsion due to charge and attraction due to dispersion. BeF_2 and MgF_2 are linear, but CaF_2 ($\theta = 140°$), SrF_2 ($\theta = 108°$) and BaF_2 ($\theta = 100°$) are bent, in addition $CaCl_2$, $CaBr_2$ and CaI_2 are all linear (*cf.* Table III). For the A which are further down the periodic table, the repulsive effects of charge interactions and A–L bonding effects do not completely dominate the attractive dispersion forces, hence the bent molecules.

AL_3

An AL_3 system can adopt one of two types of geometries: (i) tpl and planar distorted tpl, both of which are favoured by dispersion interactions of L which are large compared with the A–L bond length, and by charge interactions, and (ii) tpy which is favoured by dispersion interactions between smaller L. If the ligands vary sufficiently in size or charge then the planar distorted tpl geometry is more accurately described as a T shape.

A wide range of compounds can be cited to illustrate the effect of dispersion interactions in determining geometry. Some of the data in Table IV illustrate this, as does the success of the non-bonded radii approach of Bartell and Glidewell. The preference of bulky non-charged ligands for a trigonal planar geometry has been clearly illustrated by Glidewell with a number of NL_3 molecules with large L [8]. Another interesting illustration of preference for a planar geometry is provided by NH_3. In its ground state N–H = 1.012 Å and $\theta = 106.5°$, which is consistent with $R < 0.92$ Å (N is more electronegative than C). However, in the A_2 excited state of NH_3 some electron density has moved from the N $2p_z$-type orbital to the largely hydrogenic totally symmetric orbital. This results in an increase in the hard sphere radius of the hydrogens and a small increase in the N–H bond length to 1.08 Å. Dispersion interactions thus favour a larger bond angle, and an element of repulsive charge interaction has perhaps also been introduced. It is no surprise therefore to discover that the observed geometry of the A_2 state is trigonal planar.

T shaped geometries are least common, the best known examples being ClF_3 and BrF_3 whose bond angles are respectively (87.5°, 87.5°, 185.0°) and (86.2°, 86.2°, 187.6°). Dispersion interactions favour a pyramidal geometry for these two compounds, however the most stable geometry has one fluorine with less electron density than the other two [15], so charge interactions favour a T shape. Such a structure has a lower charge repulsion (*cf.* eqn. (14)), and is observed for these molecules because the net A–L bond energy is not significantly reduced, and may even be increased, by the unequal distribution of electron density. These mixed halide systems are far from typical compounds due to the large electronegativities of both central atoms and ligands. The actual F–Cl–F and F–Br–F bond angles indicate the influence of the dispersion interaction; the charge interaction is, by eqn. (14), minimized for a $\theta > 90°$, rather than at 87.5° and 86.2°. The distorted trigonal geometries of HgL_3^- and $Rh(P\Phi_3)_3^+$ are perhaps other examples of this phenomenon, though the Rh complex may just be the result of packing of the phosphines.

TABLE IV. Data Illustrating the Relationship between L–L Interaction Predictions and Experimental Geometries for AL_3[a]

Compound	ρ (Å)	R (Å)	Geometry favoured by		Experimental	Comment	Reference
			dispersion	charge			
Group 6 halides and hydrides							
NF_3	1.371	<1.08	$\theta < 104°$	tpl	$\theta = 102.2°$		6
PF_3	1.570	>1.08	$\theta > 87°$	tpl	$\theta = 97.8°$	charge, A–L	6
AsF_3	1.706	>1.08	$\theta > 79°$	tpl	$\theta = 96.2°$	charge, A–L	6
SbF_3	1.92	>1.08	$\theta > 68.5°$	tpl	$\theta = 87.5°$	charge, A–L	17
$SbCl_3$	2.33	>1.44	$\theta > 76°$	tpl	$\theta = 97.2°$	charge, A–L	6
PCl_3	2.04	≈>1.44	$\theta > 89°$	tpl	$\theta = 100.3°$	charge	17
PBr_3	2.20	≈>1.55	$\theta > 90°$	tpl	$\theta = 101.0°$	charge	17
PI_3	2.43	≈>1.88	$\theta > 101°$	tpl	$\theta = 102°$		17
NH_3	1.012	<0.92	$\theta < 130°$		$\theta = 106.5°$		6
PH_3	1.420	>0.92	$\theta > 81°$		$\theta = 93.3°$	A–L	6
AsH_3	1.511	>0.92	$\theta > 75°$		$\theta = 92.1°$	A–L	6
SbH_3	1.704	>0.92	$\theta > 65°$		$\theta = 91.6°$	A–L	6
Boron compounds							
BH_3	1.19	>0.92	$\theta > 101°$		tpl	A–L, see text	6
BF_3	1.307	>1.08	$\theta > 111°$	tpl	tpl		6
CH_3, $^2A_2''$	1.079	0.92	$\theta \approx 117°$		tpl		6
ScF_3	1.91	>1.08	$\theta > 69°$	tpl	tpl	charge dom.	6
Oxides							
CO_3^{2-}	1.29	≈1.13	$\theta \approx 122°$	tpl	tpl		18
ClO_3^-	1.48	<1.13	$\theta < 96°$	tpl	tpy, $\theta = 106°$	charge	18
BrO_3^-	1.64	<1.13	$\theta < 87°$	tpl	tpy, $\theta = 105.5°$	charge	18
IO_3^-	1.82°	<1.13	$\theta < 77°$	tpl	tpy, $\theta = 99°$	charge, A–L	18
$FClO_2$	1.70, 1.42		OClO ≈ 105°	?tpl	OClO = 115.2°		6
			OClF ≈ 90°		OClF = 101.7°		

[a] ρ is the A–L bond length, R is the L hard sphere radius, θ is the LAL bond angle. In the comments column, A–L means either that the experimental geometry is different from the dispersion/charge predicted one due to weaker A–L bonds in the geometry predicted by considering only L–L interactions, or that the bond angle is too small to be observed (see text). Charge indicates that charge interactions have some influence on the structure, dom = dominant, disp = dispersion.

The group six halides are helpful illustrations of the interplay of the factors which determine geometry for identical ligands. We consider first the variation of A. Both NF_3 and PF_3 geometries show the influence of charge interactions, the less electronegative P being more affected. AsF_3 cannot attain its dispersion favoured geometry due to A–L bond strength considerations (see above), and shows little less influence from charge interactions than PF_3. (As and P have about the same electronegativity but the degree of charge transfer decreases down the period.) BiF_3 has not yet been observed, possibly due to the fact that at bond angles favoured by A–L bond strength, the dispersion energy is too small to counter the destabilizing effect of the charge interactions. The effect of varying L can be examined by considering a series of phosphorous halides: as the halide gets larger and less electronegative the geometry approaches more closely the dispersion favoured geometry (*cf.* Table IV). The behaviour of the group six hydrides is very similar to that of the halides but without the charge influence.

The most stable geometry for BH_3 is calculated to be tpl with bond length of about 1.19 Å. Dispersion interactions favour a geometry with a bond angle of >101°. As charge interactions will be small, A–L bond strength is the geometry determining factor. In fact, as mentioned in section I, a planar BH_3 geometry is not sufficiently stable to be normally observed, a bridged geometry with each B in an approximately tetrahedral site is observed. This geometry has favourable dispersion interactions. AlH_3 behaves in the same manner as BH_3, however, BF_3 is observed, which reflects the effect of charge interactions which in BF_3 stabilize the tpl geometry.

The general trends in oxides are worth examining. BO_3^{3-}, CO_3^{2-}, NO_3^- are all tpl, whereas the longer bond length compounds, SO_3^{2-}, ClO_3^-, BrO_3^-, IO_3^- (see Table IV) are all pyramidal illustrating the effect of dispersion forces even in charged systems.

Three-coordinate metal complexes [19] exist for a wide variety of metals. They generally involve large ligands and adopt approximate trigonal planar geometries, which are usually planar. Some complexes

adopt non-planar geometries with bond angles larger than are possible in a tetrahedral structure. $HgBr_3^-$ is an example of a non-planar three-coordinate complex, having the Hg 0.32 Å out of the Br plane and Br–Hg–Br bond angles of between 113.3° and 125.3°.

AL_4

The possible geometries for an AL_4 system fall into the continuous series square pyramidal to square planar to tetrahedral illustrated in Fig. 5. The spy geometry enables the closest approach of the ligands so is favoured by attractive forces between small ligands. The tetrahedral geometry puts the ligands as far apart as possible for a given A–L bond length, so is favoured by repulsive interactions and large ligands.

A range of examples [17] exist which illustrate the dominance of dispersion interactions in determining the geometries of main group four-coordinate systems. Some of these are given in Table V. Charge interactions become less significant with increasing coordination number, due to the larger number of ligands sharing the electron donating or withdrawing power of one A. Thus dispersion energies seem to be the most significant factor determining geometry even for fluorine compounds in four-coordinate systems. Bartell's success in accounting for the geometry of fluorine substituted compounds using a hard sphere model illustrates this point [2]. Charge interactions cannot, however, always be ignored in charged systems such as some of the oxides and halides given in Table V. Unfortunately lack of bond length information means that we cannot be as definitive as we could for AL_2 and AL_3.

Four coordination is particularly important for some transition metals. The effects of increasing A–L bond length as one goes down the periodic table is illustrated by the series Cu(II)–Ag(II)–Au(II) and Ni(II)–Pd(II)–Pt(II) (*cf.* Table V). Ag, Au, Pd and Pt complexes are invariably planar, whereas both square planar and tetrahedral Ni complexes are found (some of which adopt either geometry depending on the circumstances) and Cu complexes are usually tetrahedral. The effect of ligand size can be seen in the Ni(II) complexes of Table V. Alkyl phosphines form square planar geometries and the bulkier aryl phosphines result in tetrahedral geometries, the change-over point being $Ni(PR\Phi_2)_2^{2+}$. $NiX_2(PR_3)_2$, X = Cl, Br, I, show analogous behaviour, the chlorine compounds being planar, the iodine compounds being tetrahedral and the Br compounds being both or either geometry. NiX_2L and NiL_2 where L is a bidentate ligand and X = Cl, Br, I, NCS or NCO also often adopt both planar and tetrahedral geometries. The length of the bite of the bidentate ligand can be a determining factor here. The significance of charge interactions is illustrated by NiX_4^- and NiX_3L^-, X = Cl, Br, I, NCS or NCO which are all tetrahedral and $Ni(CN_4)^{4-}$ which is square planar. Charge interactions can be sufficient to encourage a geometry to be tetrahedral if the dispersion energy plus A–L bond energy is not significantly different between the two geometries. However, for a small ligand which exhibits no A–L bond strain and maximum dispersion interaction in a square planar conformation the charge interactions may have no visible effect. In the context of A–L bond strain it should be noted that the bonds in square planar Ni(II) are shorter than in tetrahedral Ni(II) by about 5% due to the difference between high spin and low spin electron configurations. This serves to accentuate the bond strain in the close placked geometry compared with the tetrahedral geometry, and also the comparatively reduced dispersion interaction in the tetrahedral geometry. It does not alter the discussion given above.

AL_5

The trends in AL_5 geometry as a function of ligand size with respect to A–L bond length are illustrated in Fig. 4. The difference in dispersion energy between a square based pyramid and a trigonal bipyramid is not large, but it does influence the geometry adopted by the system as is illustrated by the fluorides in Table VI. The compounds with long A–F bond lengths and little influence from charge interactions are spy with bond angles of less than 90°, those with shorter bonds or larger Fs (due to less electronegative As) are tbp.

Various stages between the sbp and tbp geometries can be found, as the geometries can be continuously distorted into one another, for example $Co^{II}(CN)_5^{3-}$, has a distorted sbp geometry with an axial–equatorial bond angle of 97.6°. Charge interactions are presumable significant in determining this geometry with more electron density on the axial CN. $Ni^{II}(CN)_5^{3-}$ has an axial–basal bond angle of 101.0° when it adopts a distorted sbp geometry, reflecting its even shorter bond lengths compared with the Co complex. It can also be found in a tbp geometry. There is a tendency for charged ligands to be involved in tbp geometries reflecting the contribution of charge interactions. Examples of this are $CuCl_5^{3-}$, $SnCl_5^-$ and $Pt(SnCl_3)_5^{3-}$.

AL_6

Many examples of octahedral AL_6 geometries could be cited especially where A is a transition metal, as is apparent from reference to any inorganic chemistry text book (e.g. ref. 4). Octahedral six-coordination compounds where A is not a transition metal include SeX_6^{2-} and TeX_6^{2-}, X = Cl, Br, which adopt undistorted octahedral geometries. Further examples are given in Table VII. Some examples of distorted octahedra, including XeF_6, can be found for molecules whose ligands are small compared with the A–L bond length and thus favour a more

TABLE V. Data Illustrating the Relationship between L–L Interaction Predictions and Experimental Geometries for AL_4[a]

Compound	Experimental ρ (Å), θ[b]	Geometry favoured by		Comment	Reference
		dispersion	charge		
Hydrides					
CH_4	1.092, tet	$\theta \approx 115°$, tet			6
SiH_4	1.481, tet	$\theta > 77°$			6
CH_3F	1.10, 1.38, HCH = 110.6°	HCH < 122°, HCF > 73°	dist. tet	A–L, charge	6
Oxides and halides					
SiO_4^-	≈1.63, tet	spl, ?dist.	tet	charge	17
PO_4^{3-}	≈1.54, tet	spl-tet	tet		17
ClO_4^-	≈1.7, tet	spl	tet	charge	17
SF_4	≈1.58, dist. spl	spl-spy			17
$IO_2F_2^-$	I–O = 1.93, OIO = 100° IF = 2.0, FIF ≈ 180°	OIO ≈ 72°	FIF ≈ 180°	A–L	17
BrF_4^+	1.69, 2.29, θ = 93.5°	spy			17
BrF_4^-	1.89, spl	spy	tet	some charge	17
ICl_4^-	2.42–2.60, spl	$\theta \approx 73°$, spy	tet	A–L	17
$Te(CH_3)_2Cl_2$	ClTeCl ≈ 180°	CH_3's close	ClTeCl ≈ 180°		17
$TiCl_4$	2.17, tet	$\theta > 83°$	tet	charge	6
$VOCl_3$	1.57, 2.14, ClVCl = 111.3°	$\theta > 85°$	tet	charge	6
Nickel, palladium, platinum complexes					
$NiCl_4^{2-}$	2.692, tet	spy	tet	charge dom.	18
$NiBr_4^{2-}$	tet	spy	tet	charge dom.	18
NiI_4^{2-}	tet	spy	tet	charge dom.	18
$Ni(CN)_4^{2-}$	spl	spl	tet	disp. dom.	18
$NiCl_2(PMe_3)_2$	2.27, 2.28, ClNiP ≈ 75°	ClNiP ≈ 79°		disp. dom.	18
$NiCl_2(PPh_3)_2$	tet	?tet			18
$NiCl_2(PHPh_2)_3$	tbp (n.b. 5 coordinate)	tbp		tet too spaced, spl too crowded	18
$NiBr_2(PEtPh_2)_2$	spl or tet	spl–tet			17
$NiBr_2(PPh_2benzyl)_2$		spl or tet	spl–tet		17
$NiBr_2(PPh_3)_2$	tet	tet			18
$NiBr_2$(diars)	spl	?spl			18
$NiI_2(PMePh_2)_2$	tet	tet			18
$Pd/Pt(NH_3)_4^{2+}$	spl	spl			18
$Pd/PtCl_4^{2-}$	spl	spl	tet		18
$Pd/Pt(CN)_4^{2-}$	spl	spl	tet		18
$Pd/PtenCl_2$	spl	spl	?tet		18
Copper, silver, gold complexes					
$Cu(CN)_4^{3-}$	Cu–C = 2.00, tet	?	tet		18
$Cu[SC(NH_2)(CH_3)]^{4+}$	tet	tet	tet		18
$Ag[SC(NH_2)(CH_3)]^{4+}$	tet	tet	tet		18
$Au[SC(NH_2)(CH_3)]^{4+}$	not tet	?spl	tet	disp. dom.	18
$CuCl_4^{2-}$	dist. tet	spl–tet	tet		18
$CuBr_4^{2-}$	dist. tet	spl–tet	tet		18
$Ag(pyridine)_4^{2+}$	spl	?spl			18
$Ag(bipy)_4^{2+}$	spl	?spl			18
$AuCl_4^-$	spl	spl	tet		6

[a]ρ is the A–L bond length, θ is the LAL bond angle. A–L bond lengths are given in the order that the ligands appear in the molecular formula, similarly bond angles. In the comments column, A–L means either that the experimental geometry is different from the dispersion/charge predicted one due to weaker A–L bonds in the geometry predicted by considering only L–L interactions, or that the bond angle is too small to be observed (see text). Charge indicates that charge interactions have some influence on the structure, dom = dominant, disp = dispersion. [b]Some bond lengths estimated from ref. 10.

TABLE VI. Data Illustrating the Relationship between L–L Interaction Predictions and Experimental Geometries for AL_5 [a]

Compound	Experimental ρ (Å), θ [b]	Geometry favoured by		Comment	Reference
		dispersion	charge		
Halides					
XeF_5^+	$\rho_b = 1.88, \rho_a = 1.81, \theta_a = 79°, \theta_b = 88°$	$\theta \approx 73°$, spyB		disp. dom.	20
IF_5	$1.88, \theta_a = 81°$, sbpB	$\theta = 70°$		A–L	17
BrF_5	$\rho_a = 1.68, \rho_b = 1.81, \theta_a = 84°$, sbpB	$\theta = 80°$		A–L	17
ClF_5	$\rho = 1.534, \theta_a < 90°$, sbpB	$\theta = 89°$			17
VF_5	$\rho = 1.7$, tbp	$\theta > 79°$	tbp		6
NbF_5	$\rho = 1.88$, tbp	$\theta > 70°$	tbp	A–L	6
PF_5	$\rho_{eq} = 1.53, \rho_{ax} = 1.577$, tbp	$\theta > 90°$			17
TeF_5^-	$\rho_a = 1.85°, \rho_b = 1.96, \theta_a = 79°$, sbpB	$\theta = 80°$			17
$SbCl_5^{2-}$	$\rho_a = 2.36, \rho_b = 2.62, \theta_a = 85°$	$\theta > 75°$	tbp	A–L	17
$CuCl_5^{3-}$	tbp	?sbp	tbp	charge	17
$Co(CN)_5^{3-}$	$\theta_a = 97.6°$, sbpA	sbp	tbp		25
$Ni(CN)_5^{3-}$	$\rho_a = 2.17, \rho_b = 1.86, \theta = 88.6°, \theta_a = 99.0°$, sbpA	$\theta_b > 84°$	tbp	disp. dom.	17
or	$\rho_e = 1.91$ & $1.99, \rho_a = 1.84$, N–Ni–N = 173°	dist. tbp	tbp	disp. dom.	17
$CuCl_5^{3-}$	$\rho_e = 2.39, \rho_a = 2.30$, tbp	spy	tbp	charge	17
$Cu(NH_3)_2(NCS)_3^-$	2.0, 1.92, tbp, NH_3 axial	tbp			18
$CuI(bipy)_2$	2.02, Cu–I = 2.71	?tbp			18

[a] θ_b is the bond angle between basal ligands in spy geometries and θ_a between axial and basal ligands. ρ_e = equatorial bond length, ρ_a = axial bond length and ρ_b = basal bond length. sbpA denotes a square based pyramid distorted so that the central atom is above the basal plane, *i.e.* more spread out than sbp, sbpB one where the central atom is below the basal plane, *i.e.* more clustered than sbp. In the comments column, A–L means either that the experimental geometry is different from the dispersion/charge predicted one due to weaker A–L bonds in the geometry predicted by considering only L–L interactions, or that the bond angle is too small to be observed (see text). Charge indicates that charge interactions have some influence on the structure, dom = dominant, disp = dispersion. [b] Some bond lengths estimated from ref. 10.

clustered geometry than the octahedron. Isolated examples of triangular prismatic geometries exist, for example $Re(S_2C_2\Phi_2)_3$ [22] which appears to safisfy the criterion of requiring a long L–L distance compared with the M–L bond length.

The requirements for a triangular prismatic geometry are in accord with the Bailar twist rearrangement mechanism for tris-chelate complexes. The twist proceeds by elongating a trigonally distorted octahedral complex along its three-fold axis, and in the process shortening the triangular face L–L distances, to form a tpr geometry. The tpr geometry then collapses to the trigonal geometry which is the enantiomer of the starting one. Thus the transition state geometry is the most stable one possible for the required symmetry and geometry type. It is of interest in this context to consider the mechanism which was proposed for the rearrangement of an octahedral metal polyhedron of a metal cluster and which results in exactly the same product (in a labelled atom sense) as the Bailar twist [21]. The metal polyhedron mechanism proceeds by breaking one metal–metal link and joining up the two vertices opposite the broken link. This mechanism was considered favourable for the metal polyhedron because it involved a small loss of the attractive metal–metal interaction energy. An analogous mechanism in a metal complex would involve a smaller loss of dispersion energy than the Bailar twist mechanism, however, in a metal complex, there is the additional factor (which is not relevant for a metal polyhedron) of the metal–ligand bond energy to be considered. The geometry with the vertices opposite the break brought close enough to have a favourable dispersion interaction involves significant metal–ligand bond strain. Thus, although the symmetry considerations are the same for the metal polyhedron of a transition metal cluster compound and for the ligand system of a metal complex, the same rearrangement mechanisms are unlikely to be energetically feasible in the two types of compound.

A final situation where the discussions of this work might be helpful is the case of mixed ligand systems. The dispersion interactions between different ligands is of different magnitudes, so if metal–ligand bonding effects do not dominate, dispersion energy magnitudes could be the determining factor in the type of geometry observed. For example $MX_2(diket)_2$ compounds, where X is a halogen and M = Zr or Hf, adopt a *cis* conformation, as do some titanium

TABLE VII. Data for AL_6 Compounds Illustrating the Predominance of Octahedral Geometries

Compound	ρ (Å)	Geometry	Comment	Reference
$Te(OH)_6$		oct		17
$Cu(NH_3)_6^{2+}$	Cu–4N = 2.1, Cu–2N = 2.6	dist. oct	different sized Ns	18
IO_6^{5-}		oct	charge and dispersion	17
AlF_6^{3-}		oct	charge and dispersion	17
PF_6^-		oct	charge and dispersion	17
IF_6^+		oct	charge and dispersion	17
$SbBr_6^{3-}$	2.8	oct	charge and dispersion	17
$SbBr_6^-$	2.56	oct	dispersion	17
$SbBr_6$		oct	dispersion	17
$MoO_3F_3^{3-}$		oct		17
$OsO_2Cl_4^{2-}$	Os–Cl = 2.38, Os–O = 1.75	dist. oct		17
$OsCl_6^{2-}$	2.36	oct		
$ReBr_4O(H_2O)$	Re–O = 1.71, Re–Br = 0.32, Re–OH_2 = 2.32	dist. oct	not fit, so strain weakest bond	17
CrF_6^{2-}		oct		
$Co(NH_3)_6^{3+}$		oct		

derivatives. Metal–ligand bonding arguments (such as the *trans* effect) cannot account for this behaviour, however if interhalogen dispersion energies are greater than halogen-diketone interactions, then a *cis* geometry is favoured by dispersion energies.

Li_nO

The final two applications we shall make are to two series of unusual compounds, alkali metal oxides and xenon compounds. Alkali metal oxides are compounds where charge interactions are expected to be particularly significant, since, for example, when bonded to an oxygen atom a lithium molecule can be expected to be more like Li^+ than Li and the polarizability of Li^+ is 0.03 Å (see Table I). Equation (3) then suggests that charge interactions will be the dominant geometry determining factor. In accord with this Li_2O, LiOH and NaOH are linear though their analogue water is bent. Similarly the most stable geometry for Li_3O [23] is D_{3h} tpl with bond length 1.70 Å and Li_3O^+ is also tpl with bond length 1.72 Å [24, 25], despite the fact that the dispersion favoured geometry is a pyramid. The tpl geometry results from the repulsion of identical positively charged lithiums. In contrast to the ClF_3 and BrF_3 systems considered above Li_3O is not more stable in a distorted geometry which has a smaller charge repulsion than the symmetrical structure. For the lithium oxides, where strong ionic bonding is operative, such a distortion would result in a net decrease in A–L bond strength which would more than offset the stabilizing effect of the decreased charge interactions. The effect of charge interactions is also seen in the most stable geometry for Li_4O which is tetrahedral with a bond length of 1.77 Å [24].

XeL_n

Compounds of Xe present an interesting study from the point of view of geometry since the ligands are invariably strongly electronegative in order to form a bond, and one might expect an interplay of charge and dispersion interactions to determine the geometry. Charge effects will be strongest for XeL_2 systems, which is reflected in the linear geometries of both XeF_2 and KrF_2 [17], for which dispersion interactions favour very bent geometries due to their long bond lengths (1.98 and 1.87 Å respectively) compared with ligand size. XeL_4 will be less affected by charge interactions, as is illustrated by XeF_4 whose bond length is 1.95 Å and which adopts the square planar geometry favoured by dispersion interactions [17]. XeO_4 has smaller bond lengths (1.74 Å [17]) and larger ligand size, so it is no surprise that the observed geometry is tetrahedral. XeO_2F_2 is a compromise between the two limiting geometries, with O–Xe bond lengths of 1.71 Å, Xe–F of 1.9 Å, OXeO bond angle of 105.7°, FXeF angle of 174.7° and FXeO angle of 90°. XeF_5^+ and $XeOF_4$ illustrate the same trends. The XeF_5^+ geometry (where minimal charge interaction effects are expected) is a distorted sbp to enable the Fs to approach each other closely. $XeOF_4$ adopts a sbp geometry with the axial ligand being O, and Xe–O 1.70 Å, and Xe–F 1.90 Å. Similarly XeO_6^{4-} is an octahedron with bond lengths of 1.86, and the neutral XeF_6, where one would expect little charge interaction, has a slightly

distorted octahedral shape to maximize F–F dispersive interactions between small ligands.

IV. Conclusions

The geometry of AL_n systems has been studied in this work by examining the interactions between the different components of the system. The aim was to develop an approach to geometry determination that could be applied simply, and at least in principle be extended to give quantitative answers. The consequences of the hypothesis that interligand interactions were the dominant factors in determining the orientation of ligands about a central atom were explored. The result was a procedure for determining geometries. The most important factors appeared to usually be hard sphere repulsion and attractive dispersion interactions. These interactions favour geometries where the ligands are as close together as their hard sphere radii and the constraints of the number of ligands allow. The different geometries favoured for different ligand sizes are illustrated in Figs. 1–6. Thus application requires an estimate of A–L bond lengths (a typical value is sufficient for determining the shape adopted) and of L hard sphere radii (*cf.* Table II), then an application of simple trigonometry.

In many systems where L is charged, either intrinsically or due to a significant degree of electron transfer across a polar bond, then the observed geometry differs from the dispersion favoured one as a result of charge interactions. Repulsive interactions result in bond angles which are larger than those favoured by dispersion interactions.

Two additional factors must be considered before adopting the dispersion/charge favoured structure as the geometry of the system, both tend to increase the LAL bond angles. The first factor is relevant only for systems with two, or perhaps three, ligands where all valence shell electrons on A are nominally involved in bonding. In a bent geometry the A–L bond strength may be weaker than in a linear geometry as the most stable electronic configuration in a bent geometry leaves less than optimal electron density in the bonds. The second factor is relevant for systems where the dispersion/charge favoured LAL bond angle is less than 90°. This forces the electron density in the two A–L bonds to be very close together near A and interbond electron repulsion becomes a relevant consideration.

The most attractive feature of this scheme for geometry determination, apart from its simplicity, is that it applies equally well to ground states, excited states, systems with odd numbers of electrons and charged systems. The sizes of ligands and bond lengths may be more difficult to determine for excited states, but reliable estimates can generally be made. The varied applications presented in this work illustrate the application of these geometry determining principles, and suggest that the principles do in fact relate to the true nature of AL_n systems. It is envisaged that application to metal carbonyl complexes and cluster compounds will be most fruitful. Such work is currently in progress.

Acknowledgements

The help of S. M. Colwell in performing the calculations on ClF_3, BrF_3 and BeH_2 using Micromol Mark 3, IBM PC version and many fruitful discussions with P. M. Rodger are gratefully acknowledged. A.R. acknowledges the support of the Royal Commission for the Exhibition of 1851.

References

1 R. J. Gillespie and R. S. Nyholm, *Q. Rev., 11,* 339 (1975).
2 L. S. Bartell, *J. Chem. Phys., 32,* 827 (1960).
3 J. K. Burdett, 'Molecular Shapes: Theoretical Models of Inorganic Stereochemistry', Wiley, New York, 1980.
4 W. W. Porterfield, 'Inorganic Chemistry: A unified Approach', Addison-Wesley, U.S.A., 1984.
5 P. E. Schipper, *J. Phys. Chem., 90,* 2351 (1986), and refs. therein.
6 W. J. Hehre, L. Radom, P. v. R. Schleyer and J. A. Pople, 'Ab Initio Molecular Orbital Theory', Wiley, New York, 1986, and refs. therein.
7 C. G. Gray and K. E. Gubbins, 'Theory of Molecular Fluids, Vol. 1 Fundamentals', Clarendon Press, Oxford, 1984.
8 C. Glidewell, *Inorg. Chim. Acta, 12,* 219 (1975).
9 S. Green, 'Advances in Chemical Physics', Vol. 25, Interscience, New York, 1981, p. 179.
10 G. H. Aylward and T. J. V. Findlay, 'SI Chemical Data', 2nd edn., Wiley Australasia, Sydney, 1971.
11 M. Davies, 'Some Electrical and Optical Aspects of Molecular Behaviour', Pergamon, Oxford, 1965.
12 B. Bederson and E. J. Robinson, 'Advances in Chemical Physics', Vol. 10, Interscience, New York, 1966, p. 1.
13 D. W. Davies, 'The Theory of the Electric and Magnetic Properties of Molecules', Wiley, New York, 1967.
14 T. J. Lee, in preparation.
15 (a) R. D. Amos and S. M. Colwell, *Micromol Mark 3, IBM PC Version*; (b) S. M. Colwell and N. C. Hardy, *J. Chem. Educ.*, (1988), in press.
16 G. Herzberg, 'Molecular Spectra and Molecular Structure, Volume III, Electronic Spectra and Electronic Structure of Polyatomic Molecules', Van Nostrand Reinhold, New York, 1966.
17 A. F. Wells, 'Structural Inorganic Chemistry', 4th edn., Clarendon, Oxford, 1975.
18 J. C. Bailar, H. J. Emeleus, R. Nyholm and A. F. Trotman-Dickenson (eds.), 'Comprehensive Inorganic Chemistry', Vol. 3, Pergamon, Oxford, 1973.
19 P. G. Eller, D. C. Bradley and M. B. Hursthouse, *Coord. Chem. Rev., 24,* 1 (1977).

20 N. Bartlett, F. Einstein and D. F. Stewart, *J. Chem. Soc. A*, 1190 (1967).
21 A. Rodger and B. F. G. Johnson, submitted for publication.
22 R. Eisenberg and J. A. Ibers, *Inorg. Chem., 5,* 411 (1966).
23 I. Alberts, Unrestricted Møllar-Plesset 2nd order optimisation with TZ2P basis set, in preparation.
24 E. D. Simandiras, Full Møllar-Plesset 2nd order optimisation with a 5s,4p,2d/4s,2p basis set. All attempts at a C_{2v} optimization collapsed to T_d, in preparation.
25 J. A. Pople, *J. Am. Chem. Soc., 104,* 5839 (1982).